

# Explicit degradation modelling in optimal lead–acid battery use for photovoltaic systems

ISSN 1751-8687

Received on 31st January 2015

Revised on 14th October 2015

Accepted on 2nd December 2015

doi: 10.1049/iet-gtd.2015.0163

www.ietdl.org

*Amir-Sina Hamed, Abbas Rajabi-Ghahnavieh* ✉*Department of Energy Engineering, Sharif University of Technology, Tehran, Iran*✉ *E-mail: rajabi@sharif.ir*

**Abstract:** Lead–acid battery is a storage technology that is widely used in photovoltaic (PV) systems. Battery charging and discharging profiles have a direct impact on the battery degradation and battery loss of life. This study presents a new 2-model iterative approach for explicit modelling of battery degradation in the optimal operation of PV systems. The proposed approach consists of two models: namely, economic model and degradation model which are solved iteratively to reach the optimal solution. The economic model is a linear programming optimisation problem that calculates the optimal hourly battery use profile based on an assumed value of the battery degradation cost. The degradation model, in turn, gives the battery degradation cost based on the battery use profile, temperature and battery characteristics. The models are solved iteratively to finally reach to the optimal battery use considering battery degradation. The proposed approach has been applied to a 4 kWp PV system and the performance of the proposed approach were evaluated. Applicability of the proposed approach in determining the optimal storage size and the economic battery life were also shown. Advantages and the capability of the proposed approach in considering PV generation and irradiation variations were also evaluated through seasonality analysis.

## 1 Introduction

Increased energy consumption has intensified the application of renewable energy technologies including photovoltaic (PV) systems and wind turbines. Solar energy is esteemed as the most important carbon-neutral energy resource that can be used in the present as well as and in the future to supply the energy need of the developed societies [1].

The stochastic nature of renewable energy resources is a big challenge in renewable energy planning and poses various operational difficulties. Energy storage systems provide a suitable mean to cope with the mentioned challenge. With a mature technology and low price, lead–acid battery is now the most commonly used energy storage technology specifically in PV application. The benefits and applicability of lead–acid battery for PV systems were well demonstrated in the literature [2, 3]. On the other hand, difficulties and, in particular, the environmental issues associated with lead–acid batteries are well known and other battery types such as lithium-ion, NaS and NiMH are under development/improvement. Nevertheless, there are some researchers as in [4] who believe that the lead–acid battery will survive in the future.

However, battery life is limited by various degradation failures such as corrosion, sulphating, shedding of active material and gassing [5]. Battery degradation highly depends on the battery utilisation profile as the charge/discharge profiles can directly accelerate battery degradation mechanisms. Misoperation of battery in a renewable system can directly increase the battery maintenance cost and can overshadow the economic feasibility of the system. Battery management systems have been developed to control charge/discharge regimes to extend the battery life [6].

More than 100 years of lead–acid battery application has led to widespread use of lead–acid battery technology. Correctly inclusion of the battery degradation in the optimal design/operation of the lead–acid battery-assisted systems, including renewable energy system, can considerably change the economy of such systems.

However, little researches have been reported on explicit integration of battery degradation on optimal operation/design of

battery-assisted systems. In [7], an ampere–hour (Ah) throughput method has been developed to predict the lifetime of lead–acid batteries in renewable energy systems. The battery model developed in [7] has also been implemented as a software in [8] to study the battery life variations. Various battery degradation models have been discussed and evaluated in [9] for a stand-alone PV system. In [10], a techno-economic model has been presented for battery systems to determine the trade-off between the quality of service and the economic costs. A rule-based control scheme has been presented in [11] for battery charge management. An approach has been presented in [12] to determine the battery capital and operation and maintenance costs for a 4 kWp grid-connected hybrid energy system.

While battery degradation is a complicated phenomenon [7], just simplified battery life models have been incorporated in available researches to optimise battery systems design/operation. This is mainly due to the fact that battery degradation models are composed of highly non-linear complicated equations and constraints. Therefore, it is not easy to integrate such non-linear equation and constraints in an optimisation framework without facing fundamental mathematical and numerical problems regarding the problem solution and, in particular, the optimality of the results.

On the other hand, existing simplified battery degradation models cannot be used as the general models in the battery/system optimisation problems without large errors due to the approximation made in the existing models. More work is still needed to integrate full-scale battery degradation models in optimal operation/design of battery-assisted systems.

A new 2-model iterative approach has been proposed in this paper to optimise the operation of a PV-battery system in which the battery degradation was explicitly considered in full details. The proposed approach consists of two models: namely, the economic model and the degradation model.

The economic model is a linear optimisation problem that gives the optimal hourly profile of battery state-of-charge (SoC) for an assumed set of input data including the battery degradation cost. The degradation model, on the other hand, determines the battery

capacity degradation for the obtained hourly SoC profile by solving the complicated battery degradation model and gives the battery degradation cost. The models are solved consequently in several iterations until the battery degradation cost converges. Optimal battery use considering battery degradation is then obtained.

The main contributions of this paper are:

- (i) Integration of detailed battery degradation model in the optimal operation of battery-PV system.
- (ii) The 2-model iterative approach to solve both economic and degradation models while the linear optimisation guarantees the optimality of the results.
- (iii) Integration of available important degradation models and piece-wise linear approximation in the battery corrosion modelling.

While the proposed 2-model iterative approach has been used to study the lead–acid battery, it can be adopted for other battery types. However, while the degradation/failure mechanisms of the lead–acid batteries are well known, adoption of the proposed approach for other battery types requires that the degradation model for the desired battery type shall be developed to be used in the degradation model.

The rest of this paper was arranged as follows: Section 2 discusses the development and validation of the battery degradation model. Economic model has been presented in Section 3. Application of the proposed approach has been demonstrated in Section 4 while the proposed approach has been evaluated in Section 5. Concluding remarks have been presented in Section 6.

## 2 Battery degradation model

### 2.1 Concept

Battery ageing mechanisms have been well discussed in [13]. Important mechanisms resulting in battery capacity loss are generally divided into two main areas: electrodes degradation modes and electrolyte degradation modes.

Electrodes degradation also branches to manufacturing-based and operational-based degradation modes. Manufacturing-based modes are not considered in this paper. Operational degradation modes of the electrodes include sulphating, corrosion and shedding of active mass. Electrolyte-related degradation modes in lead–acid batteries include stratification and gassing [5].

The most detailed battery life model has been presented in [7] in which the basic mathematical equations for main battery degradation mechanisms have been presented. However, as the model presented in [7] is not easy to use as it is not clear in some aspect. On the basis of [7], the authors have integrated other models associated with battery degradation in [13–17] to develop a comprehensive battery degradation model. The rest of this section contains main models and equations used to evaluate the battery degradation.

The battery voltage during charge and discharge is calculated through the modified Shepherd equation as follows [7]

$$U(t) = U_{0C} - g_C \text{DoD}(t) + \rho_C(t) \frac{I(t)}{C_N} + \rho_C(t) M_C \frac{I(t)}{C_N} \frac{\text{SoC}(t)}{C_C - \text{SoC}(t)}, \quad \forall I(t) > 0 \quad (1)$$

$$U(t) = U_{0D} - g_D \text{DoD}(t) + \rho_D(t) \frac{I(t)}{C_N} + \rho_D(t) M_D \frac{I(t)}{C_N} \frac{\text{DoD}(t)}{C_D(t) - \text{DoD}(t)}, \quad \forall I(t) \leq 0 \quad (2)$$

In which,  $U(t)$  is the battery voltage;  $I(t)$  is the battery current;  $C_N$  is the battery nominal capacity;  $\text{DoD}(t)$  is the depth of discharge, where  $\text{DoD} = 1 - \text{SoC}$ ;  $C_C$  and  $C_D(t)$  are the battery capacity during charge and discharge, respectively;  $U_{0C}$  and  $U_{0D}$  are the battery open-circuit cell voltage during charge and discharge, respectively;  $g_C$  and  $g_D$  are

the electrolyte proportionality constant during charge and discharge, respectively;  $M_C$  and  $M_D$  are the charge transfer overvoltage coefficient during charge and discharge, respectively; and  $\rho_C(t)$  and  $\rho_D(t)$  are charging and discharging ohmic resistances, respectively.

During the battery life, the corrosion layer grows, leading to increase in the charging and discharging ohmic resistances.

Gassing current is calculated via Tafel approximation from the following equation [7]

$$I_{\text{Gas}} = \frac{C_N}{100 \text{ Ah}} I_{\text{Gas},0} \exp(c_U(U - U_{\text{Gas},0}) + c_T(T - T_{\text{Gas},0})) \quad (3)$$

where  $T$  is the battery temperature;  $c_U$  and  $c_T$  are the voltage and temperature coefficients; and  $I_{\text{Gas},0}$  is the nominal gassing current at the voltage  $U_{\text{Gas},0}$  and temperature  $T_{\text{Gas},0}$ .

SoC is then calculated as follows

$$\text{SoC}(t) = \text{SoC}(0) + \int_0^t \frac{I(\tau) - I_{\text{Gas}}(\tau)}{C_N} d\tau \quad (4)$$

SoC equals to 1 means that all potential lead sulphate crystals have been completely converted into the lead oxide/lead as the positive or negative electrode.

During the life of the battery, due to the loss of active material, battery discharge capacity in (2) reduces as follows [7]

$$C_d(t) = C_d(0) - C_{\text{corr}}(t) - C_{\text{deg}}(t) \quad (5)$$

where  $C_d(0)$  is the initial battery capacity;  $C_{\text{corr}}(t)$  is the corrosion capacity loss; and  $C_{\text{deg}}(t)$  is the active material degradation capacity loss.

Battery reaches the end of life when the  $C_d(t)$  capacity reaches 80% of  $C_d(0)$ .

Major issues in the calculation of  $C_{\text{corr}}(t)$  and  $C_{\text{deg}}(t)$  for (5) have been discussed in Sections 2.1 and 2.2.

### 2.2 Active material degradation

Degradation of active material occurs due to the discharge cycle of the battery. The battery equivalent discharge cycle,  $Z_W(t)$ , is obtained according to the discharge current,  $I_{\text{dch}}(\tau)$ , SoC factor,  $f_{\text{SoC}}(\tau)$  and acid stratification factor,  $f_{\text{acid}}(\tau)$ , as follows

$$Z_W(t) = \frac{1}{C_N} \int_0^t |I_{\text{dch}}(\tau)| f_{\text{SoC}}(\tau) f_{\text{acid}}(\tau) d\tau \quad (6)$$

SoC and acid stratification factors have been introduced in (6) to include the impact of adverse discharge cycles.

SoC factor depends on the time passed since the last full charge and also on the duration in which the battery has been remained at a low SoC. Mechanical stress takes place in low SoC due to the sulphate crystals growth in the battery. SoC factor is calculated as follows

$$f_{\text{SoC}} = 1 + (c_{\text{SoC},0} + c_{\text{SoC},\min}(1 - \text{SoC}_{\min}(t)|_{t_0}^t)) \times f_i(I, n) \Delta t_{\text{SoC}}(t) \quad (7)$$

$\text{SoC}_{\min}(t)$  indicates the minimum SoC since the last full charge at ( $t_0$ ) and  $f_i(I, n)$  characterises the impact of current which depends on the number of bad recharges ( $n$ ) as completely demonstrated in [7].

The acid stratification factor represents the impact of loss in the heterogeneity of sulphuric acid in the electrolyte. This factor is elucidated in the terms of integrating the differences of  $f_{\text{plus}}$  and  $f_{\text{minus}}$

$$f_{\text{stratification}} = \int (f_{\text{plus}} - f_{\text{minus}}) dt, \quad \forall f_{\text{stratification}} \geq 0 \quad (8)$$

In which  $f_{\text{plus}}$  comprises the entire elements which reduce the

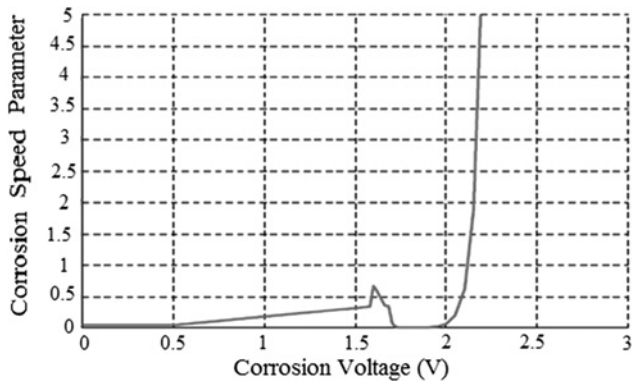


Fig. 1 Corrosion speed parameter versus corrosion voltage [14]

homogeneity of electrolyte, including low SoC since the last full charge and discharge current. On the other hand,  $f_{minus}$  represents the phenomena which lead to increase in the homogeneity of electrolyte such as gassing effect which agitates the acid and diffusion during long periods.

The acid factor is calculated as in (9) based on the discharge current in which  $I_{ref}$  represents the normalised reference current

$$f_{acid} = 1 + f_{stratification} \sqrt{\frac{I_{ref}}{|I(t)|}} \quad I(t) < 0 \quad (9)$$

It can be seen in (9) that the smaller discharge current leads to higher acid factor.

The capacity deficit due to the degradation,  $C_{deg}(t)$ , is finally calculated as follows [7]

$$C_{deg}(t) = C_{deg,lim} \exp^{-c_z(1 - (Z_W(t)/1.6Z_{IEC}))} \quad (10)$$

where  $C_{deg,lim}$  is the capacity at the end of battery life and  $Z_{IEC}$  is the number of cycles under standard condition mentioned in the battery datasheet.

### 2.3 Corrosion of positive grid

The corrosion model represents the growth in the thickness of the layer on the positive grid. The layer amplifies the grid resistance and lowers the contact of the active material to the grid. Increase in the grid resistance due to the corrosion is modelled as follows [7]

$$\rho_{corr}(t) = \rho_{corr,lim} \frac{\Delta W(t)}{\Delta W_{lim}} \quad (11)$$

In which  $\Delta W(t)$  represents the increase in the layer thickness at the time ( $t$ ) and  $\Delta W_{lim}$  denotes the maximum increase in the layer thickness at the end of battery life. The parameter  $\rho_{corr,lim}$  represents the layer specific resistance at the end of the battery life.

Corrosion speed parameter at the corrosion voltage  $U_{corr}$  and temperature  $T$ ,  $K_S(U_{corr}, T)$ , is an important factor to determine  $\Delta W(t)$  which is obtained according to the Arrhenius law [7]

$$K_S(U_{corr}, T) = K(U_{corr}) \exp(k_{S,T}(T - T_{corr,0})) \quad (12)$$

where  $K(U_{corr})$  represents the corrosion speed parameter,  $T_{corr,0}$  is the nominal corrosion temperature and  $k_{S,T}$  indicates corrosion speed temperature factor.

While no explicit relation for  $K(U_{corr})$  was available to the authors, just an experimental curve in Fig. 1 was found in an old reference [14] which shows the  $K(U_{corr})$  for the different values of  $U_{corr}$ .

On the basis of Fig. 1, the authors have developed suitable mathematical representations for  $K(U_{corr})$  as follows:

$$K(U_{corr}) = 0.2326U_{corr} - 0.0257, \quad U_{corr} < 1.74 \quad (13)$$

$$K(U_{corr}) = 0, \quad 1.74 \leq U_{corr} \leq 2 \quad (14)$$

$$K(U_{corr}) = 88.4U_{corr} - 183, \quad U_{corr} > 2 \quad (15)$$

Once  $K(U_{corr})$  is calculated using (13)–(15),  $K_S(U_{corr}, T)$  is then calculated and  $\Delta W(t)$  is obtained as explained in [14]. Battery capacity loss due to the corrosion,  $C_{corr}(t)$ , is finally calculated as in (16)

$$C_{corr}(t) = C_{corr,lim} \frac{\Delta W(t)}{\Delta W_{lim}} \quad (16)$$

$\rho_{corr,lim}$  and  $C_{corr,lim}$  are calculated as fully explained in [15].

### 2.4 Validation

In [13, 16], a compound current profile has been used for the battery degradation model validation, as shown in Fig. 2. The same current profile was used in this paper to validate the battery degradation model.

It can be seen in Fig. 2 that, at the beginning, there are five 10 A full charge currents in order to condition the battery initial capacities which then are followed by a couple of rest days. Then PV block profiles with interspersed periodic capacity tests followed.

Fig. 3 represents the simulated change in the battery capacity due to the current profile of Fig. 2. On the basis of the battery degradation model developed by the authors, the battery life is calculated as 198 days which is close to 180 days life obtained in [7] and also close to the real battery life of 239 days [15].

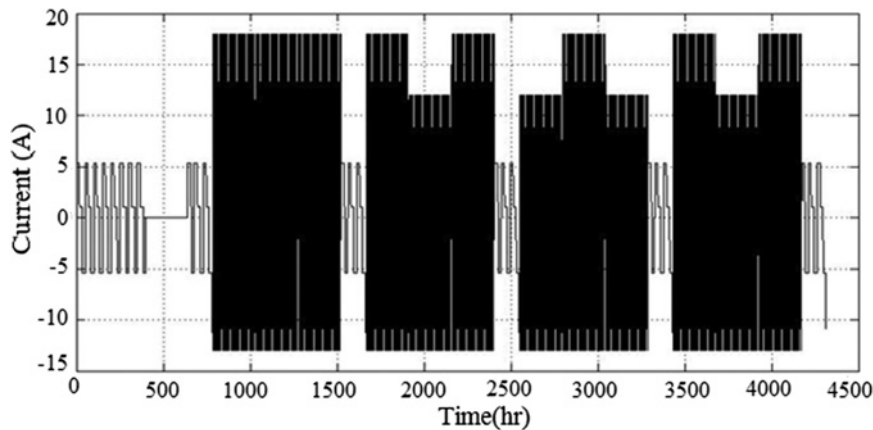


Fig. 2 Test input current profile in 200 days

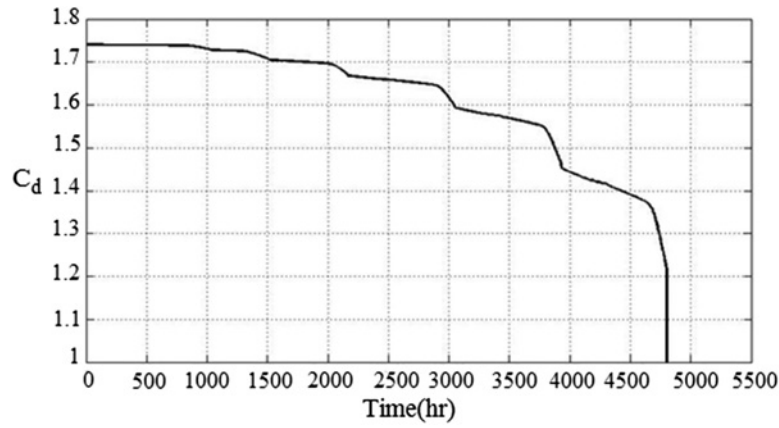


Fig. 3 Simulated capacity change

Weighted number of cycles ( $Z_w$ ) has also been verified for the developed battery degradation model and was found in good accordance with the reference results presented in [7].

Results presented in Fig. 3 and weighted number of cycles are in good accordance with the reference results on battery degradation modelling, showing that the developed battery degradation model is successful in determining the battery degradation.

### 3 Economic model

The system, as presented in Fig. 4, contains four main components including PV panels, power control system (PCS), battery system and the electric grid. PCS includes charger, inverter and control unit to charge and discharge the battery. PV panel generation can be directly sold to the grid or can be stored in the battery.

The optimising model aims to maximise total profit (TP) of selling the electricity to the grid during the operation period of operation time (OT) hours

$$TP = \sum_{t=1}^{OT} (EP(t)P_s(t) - P_d(t)BDC) \quad (17)$$

In which  $EP(t)$  is the electricity purchase price and  $P_s(t)$  is the amount of selling generation back to the grid. The battery depreciation cost (BDC) represents the battery degradation cost per the discharge power,  $P_d(t)$ .

The system power balance constraint is described as follows:

$$P_p(t) = P_c(t) - P_d(t) + P_s(t) \quad (18)$$

In which  $P_p(t)$  is the PV power generation and  $P_c(t)$  is the battery charging power.

Any growth in the battery SoC is in connection with the amount of battery charging and discharging considering charge/discharge efficiencies, battery self-discharges ( $\delta$ ) and battery nominal power ( $P_N$ ).

The constraint on the battery SoC is described as follows:

$$SoC(t+1)P_N = SoC(t)P_N + \eta_c P_c(t) - \frac{P_d(t)}{\eta_d} - \delta P_N \quad (19)$$

Since optimisation problem is supposed to reiterate, it should be terminated in a certain period of time. In (20), the difference in charging and discharging energy summation is equal to self-discharge summation applied for the operation time

$$\sum_{t=1}^{OT} P_c(t)\eta_c - \sum_{t=1}^{OT} \frac{P_d(t)}{\eta_d} = OT\delta P_N \quad (20)$$

Charging rate significantly affects battery ageing processes and the battery is supposed not to be fully charged in <3 h as follows

$$SoC(t+1) - SoC(t) \leq 0.33 \quad (21)$$

The next influential concern about the lead–acid battery is the DoD for which the high values adversely affects ageing mechanisms. Therefore, in (22), a limiting value for SoC is executed

$$SoC(t) \geq SoC_{lim} \quad (22)$$

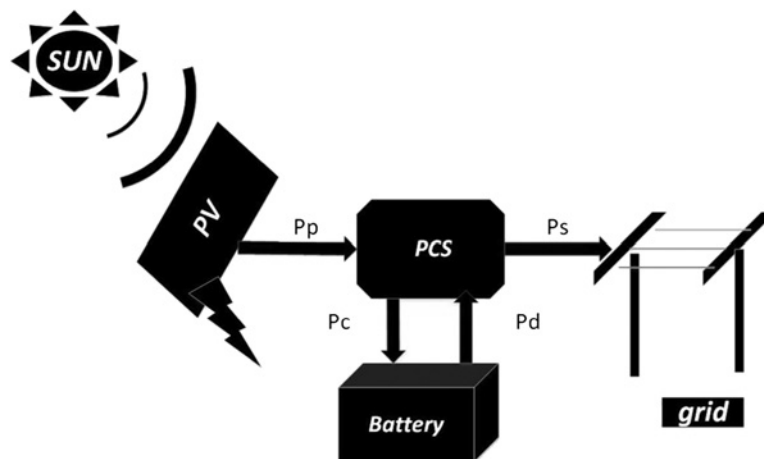


Fig. 4 Schematic design of case study

Finally, limiting values for the variables are carried out. Charging and discharging powers are bounded on the nominal energy capacity while selling the power to the grid is unbounded

$$P_d(t) \leq P_N \quad (23)$$

$$P_c(t) \geq 0 \quad (24)$$

$$P_s(t) \geq 0 \quad (25)$$

The objective function in (17) along with the constraints in (18)–(25) represents the economic model. The economic model is a linear programming problem that, once solved, gives the optimal results for the battery operation.

Total power sold (TPS), total power charged (TPC) and total power discharged (TPD) are obtained as follows

$$TPS = \sum_{t=1}^{OT} P_s(t) \quad (26)$$

$$TPC = \sum_{t=1}^{OT} P_c(t) \quad (27)$$

$$TPD = \sum_{t=1}^{OT} P_d(t) \quad (28)$$

Average indices for the system are also calculated as the average daily profit (ADP) and the average daily discharge (ADD)

$$ADP = 24 \times TP/OT \quad (29)$$

$$ADD = 24 \times TPD/OT \quad (30)$$

It should be mentioned that ADD can be used as a measure for battery usage: higher ADD means larger use of the battery.

The optimal SoC determined in the economic model is put in the battery degradation model to determine the battery capacity at the end of operation time,  $C_d(OT)$ . BDC is then obtained as follows:

$$BDC = BCL \times NB \times BUP \quad (31)$$

In which NB is the number of battery units, BUP is the battery unit price and BCL represents the amount of available battery capacity that has been consumed during the operation period, as follows:

$$BCL = \frac{C_d(0) - C_d(OT)}{C_d(0) - C_d(lim)} (\%) \quad (32)$$

Once BDC is calculated using (31), it puts again in the economic model and the optimal SoC is again calculated. BDC is again obtained using the battery degradation model. Iteration between the economic model and the degradation model continues until the variation in BDC during two consecutive iterations is <1%.

## 4 Method application

### 4.1 Case study data

The study case is a 4 kWp PV system. Daily generation profile of the PV panels is presented in Fig. 5 [17], giving the daily energy generation of 29.77 kWh.

A 3-tariff electricity purchase price is assumed for the low, medium and peak load periods, as presented in Table 1 [18].

On the basis of the generation profile in Fig. 5 and the electricity price in Table 1, without battery application, the daily profit of selling PV generation directly to the grid is obtained as 494.52 cents.

To increase the system profit, 30 units of 12 V, 54 AH lead–acid battery are used, giving a total storage capacity of 19.44 kWh. The parameters of the battery have been presented in Table 2 [7, 10].

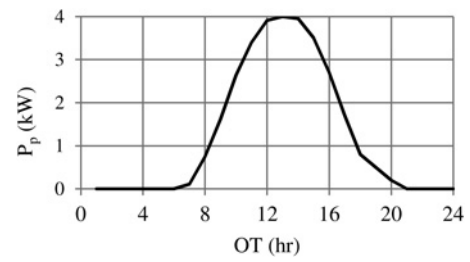


Fig. 5 Daily PV generation profile

### 4.2 Basic results

Both the economic model and the battery degradation model have been implemented in MATLAB R2013a platform on a Lenovo Z510 laptop with 2.5 GHz Intel central processing unit and 6 GB random access memory.

The proposed approach has been applied to the study case to determine the optimal battery use for the operation period of 250 days. Optimal results have been determined following four iterations between the economic model and the degradation model. Table 3 shows variation in BDC and ADP during the iterations.

It can be seen in Table 3 that BDC has reached from zero in the iteration 1 to 6 ¢/kWh in the iteration 2 which is then reduced and settled at 5.946 ¢/kWh. ADP, on the other hand, reduced in the iteration 2 and settled at the iteration 4.

It should be noted that the results obtained for the iteration 1 are associated with the BDC equals to zero. Therefore, the results obtained for iteration 1 can be considered as the results that one can obtain without considering BDC in determining optimal system operation.

Detailed results for the iteration 1 and the iteration 4 as well as those obtained for the system without battery application have been presented in Table 4.

It can be seen in Table 4 that the battery application has led to increase in TP, compared with the case in which no battery is

Table 1 Electricity purchase price

Price	Price period	Value, ¢/kWh
EP1	0–5 A.M.	10
EP2	6 A.M. to 4 P.M.	15
EP3	4 P.M. to 12 P.M.	30

Table 2 Battery parameters

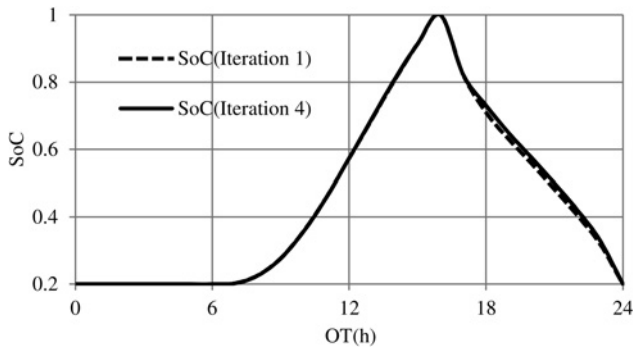
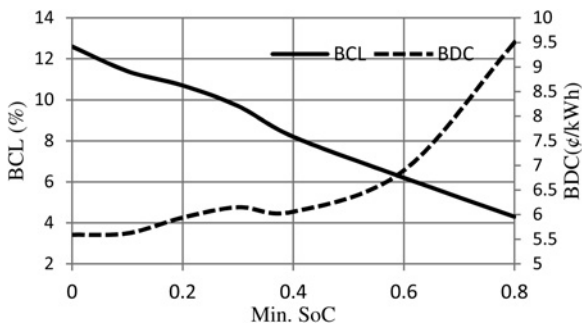
Parameter	Value	Unit
$U_{oc}$	2.18	volts
$g_c$	0.124	volts
T	300	°K
$C_N$	0.65	kWh
NB	30	units
BUP	70	\$
$\eta_c$	76	%
$\eta_d$	98	%
SoC <sub>lim</sub>	20	%
$C_d(0)$	1.75	pu
$C_c$	1.001	pu
$C_d(lim)$	1.4	pu
$\delta$	0.00694	%/h
$Z_{IEC}$	600	units

Table 3 BCD and ADP variations during iterations

Variable	Iteration 1	Iteration 2	Iteration 3	Iteration 4
BDC, ¢/kWh	0	6.008	5.9799	5.9469
ADP, ¢	647	555	556.08	556.12

**Table 4** Solution results

Variable	Iteration 1	Iteration 4	No battery
TP, \$	161, 890	139, 020	123, 630
TPC, kWh	5099	5099	—
TPD, kWh	3825	3825	—
TPS, kWh	6167	6167	7442
BDC, ¢/kWh	0	5.94	—
ADD, kWh/day	15.22	15.22	—
ADP, ¢/day	647.5	556	494.52
$C_{corr}$	0.0028	0.0028	—
$C_{deg}$	0.035	0.0347	—
$C_d$	1.7122	1.7124	—
BCL, %	10.8	10.7	—

**Fig. 6** SoC for the iteration 1 and the iteration 4**Fig. 7** BCL and BDC variations against minimum SoC

used. Inclusion of BDC in the iteration 4 has led to decrease in TP in the iteration 4 compared with the iteration 1. However,  $C_d$  calculated in the iteration 4 is greater than that obtained for the iteration 1. This shows that optimal operation obtained using the proposed approach has led to improvement in battery life while maximising the system profit.

More investigation in the results obtained for the iterations 1 and 4 has shown that  $C_{deg}$  is greater in the iteration 1 than in the iteration 4. As  $C_{deg}$  represents the capacity loss due to the active material degradation (Section 2.2), it implies that the active material degradation is smaller in the iteration 4 compared with the iteration 1. Remembering that the active material degradation is affected by the battery discharge rate, it can be concluded that battery discharge in the optimal solution (iteration 4) is smaller than that happening in the iteration 1.

Fig. 6 shows the SoC obtained for the iterations 1 and 4.

**Table 5** ADP and BDC variations with NB

Number of batteries	5	15	25	35	40	45	50	55
BDC, ¢/kWh	5.43	5.37	5.38	6.21	6.5	4.79	4.9	5.04
ADP, ¢	506.16	529.96	554.16	561	565.24	598.52	596.72	594.36

It can be seen in Fig. 6 that the SoC decline rate in the iteration 4 is smaller than that obtained for the iteration 1, confirming that the proposed approach, once fully applied, alters the battery usage to enhance the battery life.

#### 4.3 Minimum SoC impact

Battery minimum SoC in (22) is the other factor that directly affects the ADP as well as the battery degradation. Battery minimum SoC determines the amount of available battery capacity that can be used to store PV generation during the day for being sold during the afternoon. Increase of the minimum SoC leads to the decrease in the available battery capacity, resulting to decrease in ADP.

Impact of the minimum SoC has been evaluated by the proposed approach and the variations in BDC and BCL due to the changes in the minimum SoC has been presented in Fig. 7.

It can be seen in Fig. 7 that the increase in the minimum SoC has led to decrease in BCL. This shows that reducing the available battery capacity for energy storage has led to the decrease in the battery degradation. The value of numerator in BDC calculation in (31), so, decreases once minimum SoC increased. While one might expect reduction in BDC with increase in minimum SoC, it is interesting to observe in Fig. 7 that BDC has increased with minimum SoC. The reason is that, though BCL decreases with increase in the minimum SoC, the battery use by the system has been reduced as well and ADD has also been reduced.

While it is practical to imposing a limit on minimum SoC to extend the battery life [19], results obtained by the proposed approach indicate that this increases the unit cost of the battery degradation for the system. The proposed approach can be used to evaluate the impact of minimum SoC on the battery economy.

#### 4.4 Battery capacity impact

The impact of the batteries storage size has been evaluated by changing the number of battery units. Results have been presented in Table 5.

It can be seen in Table 5 that both ADP and BDC vary with NB. It can also be seen that maximum ADP was obtained for 45 battery units and the optimal number of battery units for the system under study is 45 units. This is due to the fact that, once NB has increased from 30 to 45 units, less portion of the battery capacity has been used for energy storage and the battery degradation reduces as a consequence. TPD was also greater for 45 battery units than 30 battery units, resulting in maximum ADP for 45 battery units. Deploying more than 45 battery units, however, does not have influential impact on TPD while increases the battery cost, resulting to increase in BDC and decrease in ADP.

Therefore, the proposed approach can also be used to determine the optimal number of battery units to maximise the system operation profit.

#### 4.5 Operation duration impact

Variations in ADP and BDC with the operation duration have been analysed using the proposed method. The results have been presented in Fig. 8.

It can be seen in Fig. 8 that ADP increases from 515 cents for the operation duration of 60 days, reaches the maximum value of 560 cents for the duration of 180 days and then declines to 505 cents for 450 days. BDC, on the other hand, has the minimum value for the operation duration of 180 days and increases for other values of the operation duration.

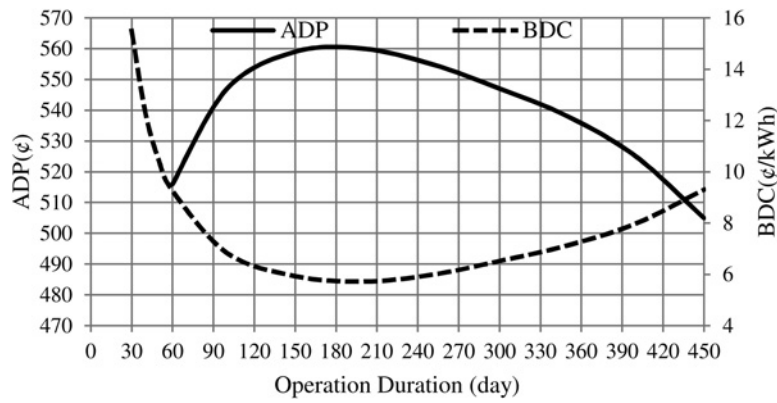


Fig. 8 Variation in BDC and ADP with operation duration

It should be noted that no optimal battery use was found for the operation duration smaller than 60 days nor for the duration >450 days. This means that it is not economic to use the battery for the operation duration smaller than 60 days or >450 days. On the other hand, BDC increases considerably for the operation duration smaller than 60 days or >450 days. This is why the proposed approach does not give the solution for the mentioned operation days and the economic model prefers not using the battery for energy storage.

The upper limit of economic operation day in Fig. 8, i.e. 450 days, is important as it shows the end of economic life of the battery. To study the economic life of the battery, the proposed approach has been applied to determine the economic life of the battery for the different values of EP3 and minimum SoC. Results have been presented in Fig. 9.

It can be seen in Fig. 9 that the battery economic life highly depends on both EP3 and minimum SoC. Higher economic life is obtained by increasing either EP3 or minimum SoC. In particular, minimum SoC has stronger impact on the economic life than EP3. However, it should be remembered that, as presented in Fig. 7, higher value for minimum SoC reduces the battery application profit to the system and increases BDC.

## 5 Analysis and discussion

### 5.1 Method comparison

The performance of the proposed approach in determining the BDC and inclusion of BDC in the system operation have been evaluated in the previous section. However, two main methods are also available to determine the BDC as follows:

- *Method 1:* Similar to the method presented in [10], BDC is determined based on the consumed battery life cycle energy

throughput as follows

$$BDC = \frac{BUP \times TPC \eta_c}{400 C_N (1 - SoC_{lim}) TPD} \quad (\text{¢/kWh}) \quad (33)$$

- *Method 2:* Constant maintenance cost for the battery life cycle is considered, as in [6], disregarding to the charge/discharge profile of the battery, as follows

$$BDC = \frac{28 \times C_N \times NB}{30 \times ADD} \quad (\text{¢/kWh}) \quad (34)$$

TPC, TPD and ADD obtained by the proposed approach have been applied in Method 1 and Method 2 to calculate BDC. Results have been presented in Table 6.

It can be seen in Table 6 that BDC obtained for the Method 1 is well higher than the one calculated by the proposed approach. On the other hand, BDC calculated for the Method 2 is so small. In particular, BDC obtained for Method 1 is so large that it does not justify the use of battery storage for PV system. This means that if the BDC obtained for Method 1 in Table 6 has been considered as the input value for an economic model, similar to the one developed in Section 3, the economic model shall opt not using the battery system and ADD will be zero.

In absence of the proposed approach, if one selects Method 1, she/he will decide not to use the battery system. On the other hand, selections of Method 2 will result in underestimation of BDC and failure in real operation of the system.

The difference between the BDCs obtained for Method 1 and Method 2 shows that the assumptions laid behind the Method 1 and Method 2 are not consistent with each other. More important, the assumptions used for Method 1 and Method 2 are neither clear

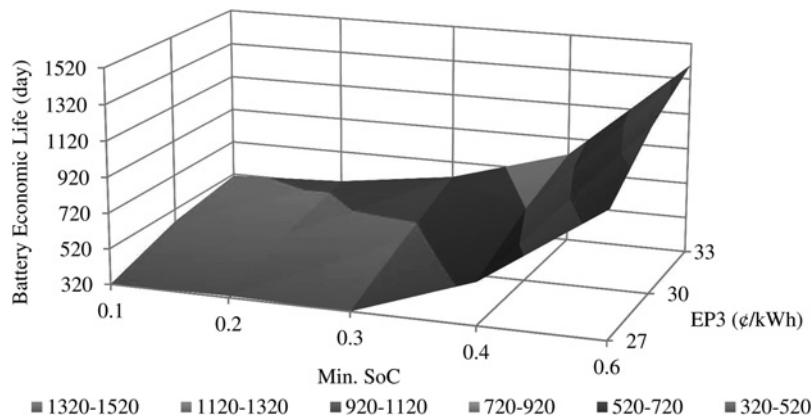


Fig. 9 Battery economic life variation

**Table 6** BDC calculation comparison

Technique	BDC, ¢/kWh
proposed approach	5.94
method 1	31
method 2	1.3

nor available and, in absence of the proposed approach, there is no clear basis to choose either of the results obtained by the methods.

On the other hand, as the results presented in the previous section has shown the battery depreciation highly depend on various technical parameters (such as operation period, minimum SoC etc.) while Method 1 and Method 2 does not consider such parameters. Therefore, while existing methods fail to precisely determine BDC on a technically sound and justifiable basis, the proposed approach can be used easily to calculate BDC in the different operating conditions.

## 5.2 Seasonality analysis

The uncertainties in both solar irradiance and ambient temperature have direct impact on the optimal operation of the system. This is due to the fact that PV generation depends highly on the solar irradiance and the battery degradation depends on the ambient temperature.

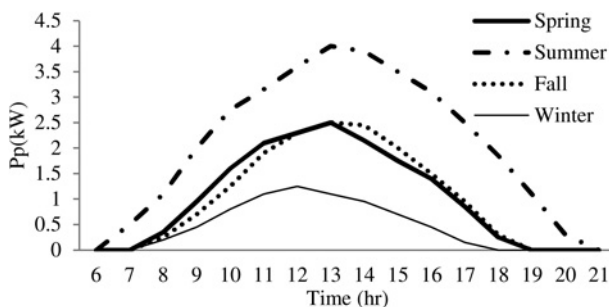
To investigate the impact of irradiance and temperature uncertainty, four seasonal scenarios have been defined which include seasonal PV generation and average ambient temperature [20]. The PV generations for the four seasons have been presented in Fig. 10.

The proposed approach has been used to study the impact of the variation in the PV generation and the ambient temperature for the battery storage system. For this analysis, 45 battery units have been considered as it was shown in Section 4.4 that the optimal battery number for the system under study is 45 units.

Table 7 presents the results obtained by the proposed approach for ADD, BDC and ADP for the four seasons. Average ambient temperature and daily PV generation associated with each season have also been mentioned in Table 7.

It can be seen in Table 7 that the values obtained for ADD, BDC and ADP varies for the four seasons of the year. In particular, it can be seen that the most profit, ADP, has been obtained for the summer which is much higher than ADP presented in Table 5 for 45 battery units. This is due the fact that daily PV generation in summer is much higher than the one associated with Fig. 5, i.e. 29.77 kWh, which was used to obtain the results presented in Table 5.

High ADD and high ambient temperature for the summer have led to smallest  $C_d$  for the summer. This is due to the fact that both battery use and high ambient temperature contribute to more degradation in the battery, leading to small  $C_d$  and large BCL. However, summer BDC is still the smallest among other seasons' and it shows that more degradation in the battery is still economic due to high PV generation.

**Fig. 10** Seasonal PV generation profiles**Table 7** Seasonal analysis results

Season (ambient temperature)	Spring (25°C)	Summer (35°C)	Fall (15°C)	Winter (5°C)
daily PV generation, kWh	16.2	33.35	16.1	7.15
ADD, kWh	11.36	20.63	10.93	5.35
$C_d$	1.7324	1.7205	1.7338	1.7373
BCL, %	5	8.4	4.6	3.6
BDC, ¢/kWh	5.61	5.25	5.35	8.58
ADP, ¢	313	685	300	119

While daily PV generations in spring and fall are so close, it can be seen in Table 7 that ADD in fall is about 4% smaller than that obtained for the spring. The reason is that low ambient temperature in fall accelerates the battery degradation and forces the proposed approach to restrict the battery use.

The largest BDC and smallest ADD were obtained for the winter as the cold ambient temperature has led to extra loss of the battery capacity. It can be seen in Table 7 that, while ADD associated with the winter is about half of the one associated with the fall, BCL associated with the winter is about 75% of the one obtained for the fall, showing that battery has degraded faster in the winter than in the fall. The largest BDC was obtained for the winter as a result.

The seasonality analysis results have shown the importance of correct modelling of PV generation and ambient temperature variation in optimal operation of battery-assisted PV system. While the existing methods, as Method 1 and Method 2, do consider neither the ambient temperature nor PV generation profile, the capability of the proposed approach in considering the variation in PV generation and ambient temperature has also been shown.

Therefore, though the proposed approach poses more computation burden to calculate BDC than existing methods such as Method 1 and Method 2 it offers more capability, more precision and more flexibility in BDC calculation. As the battery has important role in PV systems planning and operation, the application of the proposed approach in such systems is justified to clearly and precisely calculate BDC.

## 6 Conclusion

A 2-model iterative approach has been presented in this paper to calculate the BDC in the optimal operation of battery storage-assisted PV system. The proposed approach explicitly considers various parameters contributing to the battery degradation such as the temperature, charge/discharge profiles and battery characteristics. The proposed approach has been applied to a study case and the performance was evaluated. Applicability of the proposed approach in determining the optimal number of batteries in the system has been demonstrated. The impact of battery minimum SoC on the economy of battery storage application was evaluated using the proposed approach. The proposed approach can also be used to estimate economic life of the battery system according to the battery minimum SoC and electricity tariffs. A comparison between the results obtained using the proposed approach with those obtained using two other existing methods has shown that the existing methods fail to determine the BDC on a technically sound and justifiable approach. The importance of correct modelling of PV generation and ambient temperature uncertainty has also been demonstrated and the capability of the proposed approach in correctly considering the variation in PV generation and ambient temperature was also shown.

## 7 Acknowledgment

The research work for this paper has been supported by the Sharif University of Technology under the research grant no. G931031.



## 8 References

- 1 Cook, T.R., Dogutan, D.K., Reece, S.Y.: 'Solar energy supply and storage for the legacy and nonlegacy worlds', *Chem. Rev.*, 2010, **110**, (11), pp. 6474–6502
- 2 Yang, H., Wang, H., Chen, G., *et al.*: 'Influence of the charge regulator strategy on state of charge and lifetime of VRLA battery in household photovoltaic systems', *Sol. Energy*, 2006, **80**, (3), pp. 281–287
- 3 Riffonneau, Y., Bacha, S., Barruel, F., *et al.*: 'Optimal power flow management for grid connected PV systems with batteries', *IEEE Trans. Sustain. Energy*, 2011, **2**, (3), pp. 309–320
- 4 Garche, J.: 'Advanced battery systems – the end of the lead–acid battery?', *Phys. Chem. Chem. Phys.*, 2001, **3**, (3), pp. 356–367
- 5 Brik, K., Ammar, F.B.: 'Causal tree analysis of depth degradation of the lead–acid battery', *J. Power Sources*, 2013, **228**, pp. 39–46
- 6 Glavin, M., Hurley, W.G.: 'Battery management system for solar energy applications'. 41st Int. Universities Power Engineering Conf. UPEC 06, 2006, vol. 1, pp. 79–83
- 7 Schiffer, J., Sauer, D.U., Bindner, H., *et al.*: 'Model prediction for ranking lead–acid batteries according to expected lifetime in renewable energy systems and autonomous power-supply systems', *J. Power Sources*, 2007, **168**, (1), pp. 66–78
- 8 Available at <http://www.personal.unizar.es/rdufo/index.php?lang=en>, accessed November 2013
- 9 Dufo-López, R., Lujano-Rojas, J.M., Bernal-Agustín, J.L.: 'Comparison of different lead–acid battery lifetime prediction models for use in simulation of stand-alone photovoltaic systems', *Appl. Energy*, 2014, **115**, pp. 242–253
- 10 Geth, F., Tant, J., Six, D., *et al.*: 'Techno-economical and life expectancy modeling of battery energy storage systems'. Proc. 21st Int. Conf. on Electricity Distribution (CIRED), Frankfurt, 2011
- 11 Teleke, S., Baran, M.E., Bhattacharya, S., *et al.*: 'Rule-based control of battery energy storage for dispatching intermittent renewable sources', *IEEE Trans. Sustain. Energy*, 2010, **1**, (3), pp. 117–124
- 12 Giraud, F., Salameh, Z.M.: 'Steady-state performance of a grid-connected rooftop hybrid wind-photovoltaic power system with battery storage', *IEEE Trans. Energy Convers.*, 2001, **16**, (1), pp. 1–7
- 13 Culpin, B., Rand, D.A.J.: 'Failure modes of lead/acid batteries', *J. Power Sources*, 1991, **36**, (4), pp. 415–438
- 14 Lander, J.J.: 'Further studies on the anodic corrosion of lead in H<sub>2</sub>SO<sub>4</sub> solutions', *J. Electrochem. Soc.*, 1956, **103**, (1), pp. 1–8
- 15 Bindner, H., Cronin, T., Lundsager, P., *et al.*: 'Lifetime modelling of lead–acid batteries' (Risø National Laboratory, R-1515, Denmark, April 2005)
- 16 CRES: 'Results and analysis of simulated cycling tests on batteries'. Center for Renewable Energy Systems Report for a Benchmarking Project, February 2004
- 17 Mikati, M., Santos, M., Armenta, C.: 'Electric grid dependence on the configuration of a small-scale wind and solar power hybrid system', *Renew. Energy*, 2013, **57**, pp. 587–593
- 18 Borenstein, S.: 'Time-varying retail electricity prices: theory and practice', *Electr. Deregulation: Choices Chall.*, 2005, pp. 111–130
- 19 Lam, L.T., Haigh, N.P., Phyland, C.G., *et al.*: 'Failure mode of valve-regulated lead–acid batteries under high-rate partial-state-of-charge operation', *J. Power Sources*, 2004, **133**, (1), pp. 126–134
- 20 Ekren, O., Ekren, B.Y.: 'Size optimization of a solar-wind hybrid energy system using two simulation based optimization techniques', in Carriveau, R. (ed.): 'Fundamental and advanced topics in wind power' (INTECH Open Access Publisher, 2011)

Copyright of IET Generation, Transmission & Distribution is the property of Institution of Engineering & Technology and its content may not be copied or emailed to multiple sites or posted to a listserv without the copyright holder's express written permission. However, users may print, download, or email articles for individual use.